NASA TECHNICAL MEMORANDUM

NASA TM X-3541

NASA TM X-3541

COMPARISON OF THERMAL ANALYTIC MODEL WITH EXPERIMENTAL TEST RESULTS FOR 30-CENTIMETER-DIAMETER ENGINEERING MODEL MERCURY ION THRUSTER

Jon C. Oglebay

Lewis Research Center

Cleveland, Ohio 44135

NATIONAL AERONAUTICS AND SPACE ADMINISTRATION • WASHINGTON, D. C. • JUNE 1977

1. Report No.	2. Government Accession No.	3. Recipient's Catalog No.
NASA TM X-3541		

4. Title and Subtitle	5. Report Date
COMPARISON OF THERMAL ANALYTIC MODEL WITH EXPERIMENTAL TEST RESULTS FOR 30-CENTIMETER-DIAMETER ENGINEERING MODEL MERCURY ION THRUSTER	June 1977
	6. Performing Organization Code

7. Author(s)	8. Performing Organization Report No.
Jon C. Oglebay	E-9064
	10. Work Unit No.
9. Performing Organization Name and Address	506-22
Lewis Research Center National Aeronautics and Space Administration Cleveland, Ohio 44135	11. Contract or Grant No.
	13. Type of Report and Period Covered
12. Sponsoring Agency Name and Address	Technical Memorandum
National Aeronautics and Space Administration Washington, D. C. 20546	14. Sponsoring Agency Code

15. Supplementary Notes

16. Abstract

A thermal analytic model for a 30-cm engineering model mercury-ion thruster was developed and calibrated using the experimental test results of tests of a pre-engineering model 30-cm thruster. A series of tests, performed later, simulated a wide range of thermal environments on an operating 30-cm engineering model thruster, which was instrumented to measure the temperature distribution within it. As a result, both the analytic model and the thruster self-heating distribution presented in a previous report have been modified. This report describes the modified analytic model and compares analytic and experimental results for various operating conditions. Based on the comparisons, it is concluded that the analytic model can be used as a preliminary design tool to predict thruster steady-state temperature distributions for stage and mission studies and to define the thermal interfaces between the thruster and other elements of a spacecraft.

17. Key Words (Suggested by Author(s))	18. Distribution Statement
Solar electric propulsion Ion engines Mathematical models	Unclassified - unlimited STAR Category 20

19. Security Classif. (of this report)	20. Security Classif. (of this page)	21. No. of Pages	22. Price*
Unclassified	Unclassified	32	A03

* For sale by the National Technical Information Service, Springfield, Virginia 22161

COMPARISON OF THERMAL ANALYTIC MODEL WITH EXPERIMENTAL TEST RESULTS FOR 30-CENTIMETER-DIAMETER ENGINEERING MODEL MERCURY ION THRUSTER

by Jon C. Oglebay

Lewis Research Center

SUMMARY

A thermal analytic model for a 30-centimeter engineering model mercury-ion thruster was developed and calibrated using experimental test results on a pre-engineering model 30-centimeter thruster.

A series of tests were performed at Lewis to simulate a wide range of thermal environments on an operating, 30-centimeter engineering model thruster, which was instrumented to measure the temperature distribution within it. As a result, both the analytic model and the thruster self-heating distribution presented in a previous report have been modified.

This report presents a description of the modified analytic model and comparisons of the analytic and experimental results for various operating conditions. Based on the comparisons, it is concluded that the analytic model can be used as a preliminary design tool to predict thruster steady-state temperature distributions for stage and mission studies and to define the thermal interfaces between the thruster and other elements of a spacecraft.

INTRODUCTION

Missions for which the use of large ion thrusters are desired require that the thrusters operate over a wide range of power levels and thermal environments (0.3 to 5 AU) for as long as 5 years (private communication from C. G. Sauer of the Jet Propulsion Laboratory). These missions also require having a large number of thrusters, with as few as two or as many as nine thrusters operating at the same time. Because of the wide range of power levels and thermal environments, an analytic model is

required to compute the steady-state temperature distribution within the thruster as well as to predict the thermal interaction of the thruster with the environment, adjacent thrusters, and the spacecraft itself.

In addition to the model presented in reference 1, there have been thermal models developed for 20-centimeter ion thrusters (refs. 2 and 3) as well as studies on the self-heating pattern of operating 15- and 20-centimeter ion thrusters (refs. 4 and 5). In all of these studies experimental data were obtained with operating thrusters instrumented with thermocouples located in the assumed areas of thermal deposition. The analytic models and the thruster self-heating distributions were then adjusted to obtain agreement of the experimental and predicted temperatures.

This combined analytic-experimental approach has been used in this study. The experimental data were obtained with an operating, 30-centimeter engineering model ion thruster (ref. 6). The analytic model presented in reference 1, which was originally calibrated using experimental data presented in reference 7, was modified. The self-heating distribution was then adjusted to obtain satisfactory agreement with the experimentally obtained steady-state temperature distributions presented in reference 6.

Once the self-heating distribution was established, the model was used to compare the temperature distributions obtained during simulated multiple thruster operation with varied solar flux. Comparisons of the predictions of the analytic model with the data obtained during the test program presented in reference 6 will be given.

THERMAL INVESTIGATION

Thruster Thermal Characteristics

The temperature profile within the thruster is a function of the thruster design, the operating power level (i.e., beam current), and the environment in which the thruster operates. These factors determine the heat flow paths within the thruster, the amount of heat deposited within the thruster, and the sinks to which the heat is rejected.

Heating of specific thruster components may be required (e.g., in vaporizers), or may occur due to inefficiencies in the ion beam. The amount of heat supplied to the main, cathode, and neutralizer vaporizers (fig. 1) nominally varies from 2 to 7 watts each, depending on the beam current (ref. 6). Although this heat causes locally high temperatures compared with the main components of the thruster, they are so isolated that they have essentially no effect on the temperature distribution within the thruster or with the thermal interfaces with the spacecraft or environment. The same applies to the cathode and neutralizer tips.

By far the largest heat source is the discharge power. The amount of heat generated in the discharge varies from 111 to 370 watts for beam currents of 1/2 and 2 amperes, respectively (ref. 6). This energy for the most part is deposited in the dis-

charge chamber (anode, engine body, etc.), with the remainder exiting the thruster through the apertures in the screen and accelerator grids (fig. 1). This discharge power, along with the environment and thruster design, determines the temperature distribution within the thruster.

Thermal Model

The concept of treating heat flow problems in terms of electrical networks, based on the equivalence of the electrical and thermal conductance equations, is well developed (ref. 8). The concept basically involves the determination of the thermal resistance paths within a given network and then numerically determining the resulting temperature distribution.

The original thermal network (ref. 1) was reduced from 88 diffusion and 6 boundary nodes to 56 diffusion and 6 boundary nodes. A cutaway view of an engineering model thruster is shown in figure 1; the nodal layout is shown in figure 2. The nodes and materials used are shown in table I. In general, the main components of the thruster (i.e., anode, engine body, ground screen, etc.) were divided into four circumferential quadrants. This approach allows the nodes in each quadrant to see any environment desired. This capability was used to simulate multiple thruster operation by surrounding the thruster with variable temperature azimuthal shields as will be discussed later.

The main differences between this model and the original are

(1) The nodes associated with the neutralizer, cathode vaporizer, cathode, and main vaporizer assembles have been omitted. The nodal simulation of these areas was not a good representation of the actual hardware; a more detailed analytic model of these areas is required. Furthermore, as mentioned before, a previous analysis has shown that these assemblies are so isolated from the main components of the thruster that they have essentially no impact on the temperature distribution within the thruster.

(2) The number of nodes on the anode was increased from 8 to 16 (4 circumferential by 4 axial) because of the extreme temperature gradient measured during the tests.

The heat exchange within the thruster is predominately by radiation. This requires that the surface optical properties of the materials be known with a reasonable degree of accuracy. However, there can be considerable variation of the optical properties due to nonuniform surface finish, the deposition of debris from the operating thruster, and any temperature dependence of the surface properties.

Small samples of the anode and mask were removed, and their optical properties measured experimentally between wavelengths of 1 to 15 micrometers. Based on these measurements, emissivity values used in the model were 0.60 for the interior surface of the anode, 0.30 for the external surface of the mask, and 0.15 for all other thruster

surfaces. The vacuum chamber was assumed to have an emissivity of 1. For interior nodes radiating through the grids to the cold walls of the chamber, a cavity effect emissivity of 0.275 was used for the baseplate, and the anode emissivity varied from 0.675 to 0.8, depending on the location of the nodes. These values were based on data presented in reference 9.

The radiation exchange factor $\mathcal{F}_{ij}$ was approximated by the following relationship developed in reference 8:

$$\mathcal{F}_{ij} = \frac{1}{\left(\frac{1}{\epsilon_i} - 1\right) + \frac{A_i}{A_j}\left(\frac{1}{\epsilon_j} - 1\right) + \frac{1}{F_{ij}}}$$

where ϵ_i and ϵ_j are the emissitivities of the i^{th} and j^{th} nodes, A_i and A_j are the radiating areas of the i^{th} and j^{th} nodes, and F_{ij} is the geometric configuration factor from the i^{th} to the j^{th} node. The values of F_{ij} were calculated either by hand or numerically using the computer program in reference 10. These inputs were then used to calculate the radiation conductor values between the nodes.

Although radiation is the dominant means of heat transfer within the thruster, the linear conduction contribution cannot be overlooked. Therefore, it is necessary that the thermal conductivity of the materials as well as the contact conductance across joints be known. The thermal conductivities of the materials are well documented in the literature and are relatively constant over the temperature range of concern. The values for thermal conductivity used herein are presented in table II. Estimating the contact conductance across joints is a more difficult task. The conductance between the supports connecting the engine body with the anode and ground screen were neglected because the contact area is very small compared with the surface area of the nodes. Reducing the heat transfer (i.e., thermal conductivity), to estimate joint conductance between other nodes, had essentially no effect on the temperature distribution within the thruster. Therefore, joint conductance was neglected in the model. It was also assumed that there was no heat transfer between the ground screen and the rear shield because of the very poor contact in that area.

The program chosen to solve the analytical model was the systems improved numerical differencing analyzer, or SINDA, which is a thermal analyzer program described in reference 11. Once the necessary model information was obtained, it was coded in SINDA format, and the steady-state temperature distributions of the thruster were calculated. Predicting variations in the thermal performance of the thruster due to property changes can be done with relative ease.

Thruster Self-Heating Distribution

When the thruster is operating, there are significant heat inputs to various thruster components from ion, electron, and plasma radiation heating. The distribution of this heat in the thruster is not known precisely and presents another uncertainty in a purely analytical approach.

The approach taken here was initially to assume that the heat distribution to the various components of the thruster was the same as that used in reference 1 for a 2-ampere beam current. However, in this series of tests (ref. 6) there was a thermocouple located 1.27 centimeters (1/2 in.) from the grid end of the anode (front) and one located 1.27 centimeters (1/2 in.) from the baseplate end of the anode (rear). The tests showed a very sharp temperature gradient from the back to the front of the anode. This gradient was undetected in earlier tests because of the lack of instrumentation that close to the front of the anode except for one data point (presented in ref. 7) where the measured temperature was 655 K. Because of the sharp temperature gradient, the initial heating distribution assumed yielded very poor agreement especially in the anode area. It was therefore necessary to remodel the anode, as mentioned previously, before making any further attempts to estimate the heating distribution within the thruster.

After the anode was remodelled, the initial heating distribution was adjusted until satisfactory agreement between analytic and experimental temperatures was attained for a 2-ampere beam current. The same ratios were then applied for beam currents of 1 and 1/2 ampere. The final values and percentages of the total heat input to the various components for the three beam currents are shown in table III along with the total discharge power. The total heat input is less than the total discharge power because some heat escapes through the apertures in the grids.

As can be seen, the majority of the heat goes to the front of the anode (59 percent); whereas in references 1 and 2, only 18 percent was assumed to reach the front of the anode. The values for the other components of the thruster are as much as a factor of 5 less than the distributions presented in references 1 and 2. Based on the above comparisons, it appears that the thrusters are not heated as uniformly as has been presented in the past. It is felt, however, that the approximations in table II can be used for other size thrusters of the divergent magnetic field type.

RESULTS AND DISCUSSION

Calibration Tests

The analytic model was calibrated using data for a 2-ampere beam current for a single thruster in a vacuum chamber surrounded by liquid-nitrogen-cold walls both with

and without simulated solar flux. To be acceptable, the analytic model temperatures were to agree to within ±10 percent of the experimental results. This level of accuracy was chosen because the temperatures are not near the material limits and, therefore, better accuracy is not required for the safety of the thruster. Also, this level of accuracy characterizes the thruster as an element of a spacecraft. Once the heating distribution shown in table III was established for 2 amperes and no solar incidence, runs were made using the distributions for 1- and 1/2-ampere beam currents. These beam currents represent full, half, and quarter power.

The comparison of experimental and analytic temperature distributions for these three beam currents are shown in table IV. Shown on this and ensuing tables are the experimental and analytic temperatures, the percent error between the two, and the average of the absolute values of the errors not including the rear shield. All of the analytic predictions are well within 10 percent of the experimental results, with the average absolute error ranging from 2.64 percent at 2 amperes to 4.26 percent at 1/2 ampere. Generally, the calculated values are less than the measured values. The largest errors are generally in the ground screen temperatures at a 2-ampere beam current. As can be seen, the 2-ampere-beam-current model overpredicts the temperature by as much as 29 K, the 1-ampere beam current model is within the accuracy limits, and the 1/2-ampere beam current model underpredicts the temperature by as much as 14 K. These differences could be due to uncertainties in estimating view factors and effective radiating areas for curved, perforated surfaces, difficulties in measuring accurate temperatures, or some other phenomena. In any case, the ground screen temperatures are at least 100 K lower than the other components, and the errors are tolerable. As will be shown later, when the thruster is enclosed by a shield and the temperatures are much warmer, the differences sharply decrease.

The error in the rear of the engine body and the anode temperatures increase with decreasing beam current, indicating that perhaps the self-heating distribution is not directly proportional to the discharge power. The model consistently underpredicts the mask temperature. The reason for this is probably that the emissivity could vary substantially around the mask, as was indicated by visual inspection of the thruster. (The emissivity of the mask sample measured in one location was approximately 0.3.)

The rear shield temperatures were set to the average experimental values because of the complex nature of the support structure and instrumentation leads, etc. (refs. 6 and 7). Attempts were made to estimate the heat rejection from the rear shield. However, the model experienced convergence problems for most cases, and the effort was abandoned. For the cases that converged an apparent rear shield emissivity of approximately 0.40 yielded satisfactory results. However, in a more realistic situation, the environment the rear shield would view probably would not be as cluttered with support structure, instrumentation leads, etc., and the rear shield interaction with that en-

vironment could be incorporated in the model.

In order to establish the effective solar absorptivity of those components of the thruster that were subjected to solar incidence (i.e., mask, accelerator grid, and baseplate), the model was calibrated with a 2-ampere beam current and the same self-heating distribution as before but with a solar incidence of 2 suns axially on the grid end (front) of the thruster. Initially, the values of solar absorptivity used were typical handbook values for the materials. These values were later adjusted to obtain satisfactory results. It was assumed that half of the solar flux incident on the grid area went through the holes to the baseplate because the grids open area was 50 percent. Table V shows the solar heating distribution to the thruster and the assumed values of solar absorptivity used in these studies. The values of the solar absorptivities are all within 25 percent of the initial handbook quoted values used for the thruster materials.

A comparison of the experimental and analytic temperatures for the three beam currents are shown in table VI. As in the cases with no solar flux, the analytic predictions are well within 10 percent of the experimental results, except for the ground screen temperature, although they were a little higher than the no solar flux cases. The average absolute error ranges from 4.16 percent at 2 amperes to 6.22 percent at 1/2 ampere. The model consistently overpredicts the ground screen temperatures. The probable reason for this (in addition to the other possibilities mentioned earlier) is that the assumed conductive heat transfer between the ground screen and the mask is probably too high. No attempt was made to determine the sensitivity of the ground screen temperature to the conductive heat-transfer value because the disagreement, again, sharply decreases when a shield is around the thruster.

Comparing tables IV and VI, the largest increase in temperature due to the solar flux occurs on the mask, which is a solid area directly facing the solar source. The analytical increase in mask temperature is 20 to 30 K greater than the experimental increase, depending on the beam current. As the beam current decreased, the increase in temperature became greater not only for the mask, but for the other components of the thruster as well. Omitting the ground screen and mask temperatures, the average experimental increases in component temperature were 30, 34, and 53 K for beam currents of 2, 1, and 1/2 ampere, respectively, while the analytic increases were 23, 29, and 49 K. The solar flux was more in evidence at the lower beam currents because the thruster was cooler due to the lower discharge power.

Multiple Thruster Simulation

After the model was calibrated, it was compared with an experimental simulation of multiple thruster operation. Multiple thruster arrays were simulated by surrounding the

thruster with two different variable temperature azimuthal shields. The first configuration had the thruster completely surrounded by a shield as shown in figure 3; the second configuration had the thruster surrounded by a 270° shield with the neutralizer quadrant open to the vacuum chamber walls (fig. 4). These shields allowed the thruster to radiate primarily to a warm body rather than the liquid-nitrogen-cold walls. This would permit a thermal evaluation of an operating thruster surrounded by either operating or nonoperating thrusters. The shields were instrumented with thermocouples to monitor the shield temperatures. Strip heaters were attached uniformly to the bottom of the shields to control the temperature. Samples of the heater were removed, and optical property measurements made on the surface facing the thruster. The resultant emissivity was approximately 0.60. This value was used in the analysis.

The thruster was operated at the same beam currents as in the calibration tests, both with no solar incidence and with up to 2 suns of solar incidence. A series of 15 tests, 5 each at the three beam currents, were compared with analytic predictions. A comparison of the results for the 2-ampere beam current are shown in table VII. All of the analytic temperatures are well within 10 percent of the experimental values, including the ground screen, which indicates that the interaction between the ground screen and chamber environment is not being treated correctly without the shields around the thruster. In fact, the errors in the analytic predictions for the most part are lower than for the calibration cases. The maximum average absolute error is 1.55 percent, with the largest error in these cases occurring on the front of the anode.

The only major differences between these shielded cases and the calibration cases are the much better ground screen agreement and the higher (due to the presence of the shields) thruster temperatures. The temperature around the thruster, excluding the grid end, was increased from liquid-nitrogen temperature (80 K) to nearly the thruster temperature (500 K). This essentially eliminated the heat transfer from the sides of the thruster to the environment. This 420 K increase caused a maximum average experimental thruster temperature rise, excluding the ground screen, the front of the anode, and the rear shield, of only 68 K in the 360° shield case with 2 suns. The corresponding analytic temperature rise was 59 K. This means that the main heat-rejection mechanism is by radiation out of the accelerator end of the thruster to the cold walls of the chamber.

Similar results for the 1- and 1/2-ampere beam currents are shown in tables VIII and IX, respectively. As in the calibration tests, the errors generally increase with decreasing beam current but still remain well within 10 percent.

The temperature comparisons of the experimental and analytic results for the 2-ampere beam current are also given in figures 5 to 11. In these figures the average temperatures of the engine body and ground screen presented in tables IV and VI and VII are shown.

A computer listing of the SINDA input, execution procedure, and output for a typical run with a 2-ampere beam current is presented in the appendix. It should be noted that all input values are in English units because SINDA requires that the input temperatures be in degrees Fahrenheit for problems involving radiation.

CONCLUSIONS

An analytic thermal network for a 30-centimeter engineering model mercury-ion thruster has been modified and calibrated against experimental data obtained on an operating 30-centimeter engineering model thruster. Experimental data were generated at full, half, and quarter beam currents over a wide range of thermal environments. Comparisons of the analytic and experimental temperatures show that the analytic model agrees well, within 10 percent of the experimental results (about 4 percent on the average), for the main components of the thruster.

From the results of this study, it was concluded that

1. A realistic thermal model has been constructed to represent the thruster temperature distribution with an expected accuracy of 10 percent.

2. Heat losses to various components of the thruster from the plasma are much different from those previously estimated.

3. The model can be used to analyze interactions between thruster arrays, thermal environment, and the spacecraft itself.

4. The model can be used for preliminary design, flight performance, and other applications.

5. The main heat rejection mechanism is by radiation out of the accelerator end of the thruster.

Lewis Research Center,
National Aeronautics and Space Administration,
Cleveland, Ohio, March 16, 1977,
506-22.

APPENDIX - SAMPLE OF SINDA INPUT, EXECUTION PROCEDURE, AND OUTPUT

SINDA Input

```
BCD 3THERMAL SPCS
BCD 9 30 CM. EMT MODEL (NO HEATER)
END
BCD 3NODE DATA
REM
REM NODE NUMBER, INITIAL TEMPERATURE (F), AND NODE
REM THERMAL CAPACITY (BTU/F), NEGLECTED IN STEADY STATE
REM
     101,80.,.0018, 102,80.,.0018, 103,80.,.0018, 104,80.,.0018
     105,80.,.0023, 106,80.,.0023, 107,80.,.0023, 108,80.,.0023
     109,80.,.0023, 110,80.,.0023, 111,80.,.0023, 112, 80.,.0023
     113,80.,.0018, 114,80.,.0018, 115,80.,.0018, 116,80.,.0018
     9,80.,.0609, 10,80.,.0609, 11,80.,.0609, 12,80.,.0609
     13,80.,.0100, 14,80.,.0100, 15,80.,.0100, 16,80.,.0100
     17,80.,.0116, 18,80.,.0116, 19,80.,.0116, 20,80.,.0116
     21,80.,.03024, 22,80.,.03024, 23,80.,.03024, 24,80.,.03024
     25,80.,.05316, 26,80.,.05316, 27,80.,.05316, 28,80.,.05316
     29,80.,.0255, 30,80.,.0255, 31,80.,.0255, 32,80.,.0255
     33,80.,.0132, 34,80.,.0132, 35,80.,.0132, 36,80.,.0132
     37,80.,.0048, 38,80.,.0048, 39,80.,.0048, 40,80.,.0048
REM REAR SHIELD BOUNDARY NODE (F)
     -46,211.,0.
     74,80.,.0425, 75,80.,.0425, 76,80.,.0425, 77,80.,.0425
     85,80.,.0107, 86,80.,.0107, 87,80.,.0107, 88,80.,.0107
REM ENVIRONMENTAL BOUNDARY NODES (F)
     -501,-310.,0., -502,-310.,0., -503,-310.,0., -504,-310.,0.
     -505,-310.,0.
END
```

RELATIVE NODE NUMBERS — ACTUAL NODE NUMBERS

1 THRU 10	101	102	103	104	105	106	107	108	109	110
11 THRU 20	111	112	113	114	115	116	9	10	11	12
21 THRU 30	13	14	15	16	17	18	19	20	21	22
31 THRU 40	23	24	25	26	27	28	29	30	31	32
41 THRU 50	33	34	35	36	37	38	39	40	74	75
51 THRU 60	76	77	85	86	87	88	46	501	502	503
61 THRU 62	504	505								

NODE ANALYSIS... DIFFUSION = 56, ARITHMETIC = 0, BOUNDARY = 6, TOTAL = 62

```
BCD 3CONDUCTOR DATA
REM
REM LINEAR CONDUCTOR NUMBER, CONNECTING NODES AND VALUE (BTU/HR.F)
REM
     300,101,105,102,106,103,107,104,108,109,113,110,114,111,115
     112,116,.0322
     301,105,109,106,110,107,111,108,112,.0161
     3001,101,102,102,103,103,104,104,101,113,114,114,115,115,116
     116,113,.0004
     3002,105,106,106,107,107,108,108,105,109,110,110,111,111,112
     112,109,.0006
     302,9,10,10,11,11,12,12,9,.00928
     303,13,14,14,15,15,16,16,13,.00742
     305,9,13,10,14,11,15,12,16,.0399
     306,9,74,10,75,11,76,12,77,.0377
     307,13,17,14,18,15,19,16,20,.1795
     308,17,21,18,22,19,23,20,24,.141
```

```
     309,17,18,18,19,19,20,20,17,.01095
     310,21,22,22,23,23,24,24,21,.068
     311,25,26,26,27,27,28,28,25,.074
     312,29,30,30,31,31,32,32,29,.0184
     313,33,34,34,35,35,36,36,33,.0372
     314,33,37,34,38,35,39,36,40,.29
     315,37,38,38,39,39,40,40,37,.009
     338,74,75,75,76,76,77,77,74,.0046
REM  GROUND SCREEN DISCONNECTED FRM REAR SHIELD
     347,33,46,34,46,35,46,36,46,0.
     348,9,29,10,30,11,31,12,32,.0145
     349,37,85,38,86,39,87,40,88,.106
     350,85,86,86,87,87,88,88,85,.0053
REM
REM  INTERNAL RADIATION CONDUCTOR NUMBER, CONNECTING NODES,
REM  VALUE INDICATOR, 1.- CONNECTED, 0.- NOT CONNECTED
REM  ACTUAL VALUE CALCULATED LATER
REM
     -401,101,102,102,103,103,104,104,101,113,114,114,115,115,116
     116,113,1.
     -402,105,106,106,107,107,108,108,105,109,110,110,111,111,112
     112,109,1.
     -403,101,103,102,104,113,115,114,116,1.
     -404,105,107,106,108,109,111,110,112,1.
     -405,101,105,109,113,102,106,110,114,103,107,111,115,104,108
     112,116,1.
     -406,105,109,106,110,107,111,108,112,1.
     -407,101,106,102,107,103,108,104,105,113,110,114,111,115,112
     116,109,102,105,103,106,104,107,101,108,114,109,115,110
     116,111,113,112,1.
     -408,101,107,102,108,103,105,104,106,113,111,114,112,115,109
     116,110,1.
     -409,105,110,106,111,107,112,108,109,106,109,107,110,108,111
     105,112,1.
     -410,105,111,106,112,107,109,108,110,1.
     -411,101,109,102,110,103,111,104,112,113,105,114,106,115,107
     116,108,1.
     -412,101,110,102,111,103,112,104,109,113,106,114,107,115,108
     116,105,101,112,102,109,103,110,104,111,113,108,114,105
     115,106,116,107,1.
     -413,101,111,102,112,103,109,104,110,113,107,114,108,115,105
     116,106,1.
     -414,101,113,102,114,103,115,104,116,1.
     -415,101,114,102,115,103,116,104,113,101,116,102,113,103,114
     104,115,1.
     -416,101,115,102,116,103,113,104,114,1.
     -417,101,17,102,18,103,19,104,20,1.
     -418,105,17,106,18,107,19,108,20,1.
     -419,109,17,110,18,111,19,112,20,1.
     -420,113,17,114,18,115,19,116,20,1.
     -421,101,18,101,20,102,17,102,19,103,18,103,20,104,17,104,19,1.
     -422,105,18,105,20,106,17,106,19,107,18,107,20,108,17,108,19,1.
     -423,109,18,109,20,110,17,110,19,111,18,111,20,112,17,112,19,1.
     -424,113,18,113,20,114,17,114,19,115,18,115,20,116,17,116,19,1.
     -425,101,19,102,20,103,17,104,18,1.
     -426,105,19,106,20,107,17,108,18,1.
     -427,109,19,110,20,111,17,112,18,1.
     -428,113,19,114,20,115,17,116,18,1.
     -429,101,21,102,22,103,23,104,24,1.
```

```
-430,105,21,106,22,107,23,108,24,1.
-431,109,21,110,22,111,23,112,24,1.
-432,113,21,114,22,115,23,116,24,1.
-433,101,22,101,24,102,21,102,23,103,22,103,24,104,21,104,23,1.
-434,105,22,105,24,106,21,106,23,107,22,107,24,108,21,108,23,1.
-435,109,22,109,24,110,21,110,23,111,22,111,24,112,21,112,23,1.
-436,113,22,113,24,114,21,114,23,115,22,115,24,116,21,116,23,1.
-437,101,23,102,24,103,21,104,22,1.
-438,105,23,106,24,107,21,108,22,1.
-439,109,23,110,24,111,21,112,22,1.
-440,113,23,114,24,115,21,116,22,1.
-441,101,29,102,30,103,31,104,32,1.
-442,105,29,106,30,107,31,108,32,1.
-443,109,29,110,30,111,31,112,32,1.
-444,113,29,114,30,115,31,116,32,1.
-445,101,30,101,32,102,29,102,31,103,30,103,32, 104,31,104,29,1.
-446,105,30,105,32,106,29,106,31,107,30,107,32,108,31,108,29,1.
-447,109,30,109,32,110,29,110,31,111,30,111,32,112,31,112,29,1.
-448,113,30,113,32,114,29,114,31,115,30,115,32,116,31,116,29,1.
-449,101,31,102,32,103,29,104,30,1.
-450,105,31,106,32,107,29,108,30,1.
-451,109,31,110,32,111,29,112,30,1.
-452,113,31,114,32,115,29,116,30,1.
-461,101,9,102,10,103,11,104,12,1.
-462,105,9,105,10,107,11,108,12,1.
-463,109,9,110,10,111,11,112,12,1.
-464,113,9,114,10,115,11,116,12,1.
-465,101,10,101,12,102,9,102,11,103,10,103,12,104,9,104,11,1.
-466,105,10,105,12,106,9,106,11,107,10,107,12,108,9,108,11,1.
-467,109,10,109,12,110,9,110,11,111,10,111,12,112,9,112,11,1.
-468,113,10,113,12,114,9,114,11,115,10,115,12,116,9,116,11,1.
-469,113,13,114,14,115,15,116,16,1.
-470,109,13,110,14,111,15,112,16,1.
-471,113,14,113,16,114,13,114,15,115,14,115,16,116,13,116,15,1.
-472,109,14,109,16,110,13,110,15,111,14,111,16,112,13,112,15,1.
-1029,17,29,18,30,19,31,20,32,1.
-1030,17,31,18,32,19,29,20,30,1.
-1031,17,30,17,32,18,29,18,31,19,30,19,32,20,31,20,29,1.
-1034,17,21,18,22,19,23,20,24,1.
-1035,17,22,17,24,18,21,18,23,19,22,19,24,20,23,20,21,1.
-1036,17,23,18,24,19,21,20,22,1.
-1037, 17,18,18,19,19,20,20,17,1.
-1038,17,19,18,20,1.
-1039,21,29,22,30,23,31,24,32,1.
-1040,21,30,21,32,22,29,22,31,23,30,23,32,24,31,24,29,1.
-1041,21,31,22,32,23,29,24,30,1.
-1045,13,85,14,86,15,87,16,88,1.
-1046,25,86,25,88,26,85,26,87,27,86,27,88,28,87,28,85,0.
-1047,21,25,22,26,23,27,24,28,1.
-1052,17,13,18,14,19,15,20,16,1.
-1053,17,14,17,16,18,13,18,15,19,14,19,16,20,13,20,15,1.
-1054,9,33,10,34,11,35,12,36,1.
-1055,13,37,14,38,15,39,16,40,1.
-1056,13,9,14,10,15,11,16,12,1.
-1063,29,46,30,46,31,46,32,46,1.
-1122,74,13,75,14,76,15,77,16,1.
-1123,74,14,74,16,75,13,75,15,76,14,76,16,77,15,77,13,1.
-1124,74,37,75,38,76,39,77,40,1.
-1125,74,38,74,40,75,37,75,39,76,38,76,40,77,39,77,37,1.
```

```
     -1143,13,40,15,40,1.
     -1144,9,36,11,36,1.
     -1145,13,38,14,37,14,39,15,38,16,37,16,39,1.
     -1146,9,34,10,33,10,35,11,34,12,33,12,35,1.
REM
REM EXTERNAL RADIATION CONDUCTOR NUMBER, CONNECTING NODES,
REM VALUE INDICATOR
REM
     -2000,101,505,102,505,103,505,104,505,1.
     -2001,105,505,106,505,107,505,108,505,1.
     -20011,109,505,110,505,111,505,112,505,1.
     -20012,113,505,114,505,115,505,116,505,1.
     -2002,9,501,1.
     -2003,10,502,1.
     -2004,11,503,1.
     -2005,12,504,1.
     -2006,13,501,1.
     -2007,14,502,1.
     -2008,15,503,1.
     -2009,16,504,1.
     -2010,17,505,18,505,19,505,20,505,1.
     -2011,21,505,22,505,23,505,24,505,0.
     -2012,25,505,26,505,27,505,28,505,1.
     -2013,29,505,30,505,31,505,32,505,1.
     -2014,33,501,1.
     -2015,34,502,1.
     -2016,35,503,1.
     -2017,36,504,1.
     -2018,37,501,1.
     -2019,38,502,1.
     -2020,39,503,1.
     -2021,40,504,1.
     -2041,85,505,86,505,87,505,88,505,1.
     -2043,33,502,1., -2044,33,504,1., -2045,34,501,1.
     -2046,34,503,1., -2047,35,502,1., -2048,35,504,1.
     -2049,36,503,1., -2050,36,501,1., -2051,37,502,1.
     -2052,37,504,1., -2053,38,501,1., -2054,38,503,1.
     -2055,39,502,1., -2056,39,504,1., -2057,40,503,1.
     -2058,40,501,1.
     -2059,33,505,34,505,35,505,36,505,1.
     -2065,9,505,10,505,11,505,12,505,1.
     -2066,13,505,14,505,15,505,16,505,1.
     -2067,74,505,75,505,76,505,77,505,1.
     -2070,37,505,38,505,39,505,40,505,1.
     -2071,85,501,86,502,87,503,0.
     -2072,88,504,0.
     -2073,74,501,75,502,76,503,1.
     -2074,77,504,1.
END
```

RELATIVE CONDUCTOR NUMBERS			ACTUAL CONDUCTOR NUMBERS									
1	THRU	10	300	301	3001	3002	302	303	305	306	307	308
11	THRU	20	309	310	311	312	313	314	315	316	317	318
21	THRU	30	319	350	401	402	403	404	405	406	407	408
31	THRU	40	409	410	411	412	413	414	415	416	417	418
41	THRU	50	419	420	421	422	423	424	425	426	427	428
51	THRU	60	429	430	431	432	433	434	435	436	437	438
61	THRU	70	439	440	441	442	443	444	445	446	447	448
71	THRU	80	449	450	451	452	461	462	463	464	465	466
81	THRU	90	467	468	469	470	471	472	1029	1030	1031	1032
91	THRU	100	1035	1036	1037	1038	1039	1040	1041	1045	1046	1047
101	THRU	110	1052	1053	1054	1055	1056	1093	1122	1123	1124	1125
111	THRU	120	1143	1144	1145	1146	2000	2001	20011	20012	2002	2003
121	THRU	130	2004	2005	2006	2007	2008	2009	2010	2011	2012	2013
131	THRU	140	2014	2015	2016	2017	2018	2019	2020	2021	2041	2043

```
  141  THRU    150          2044    2045    2046    2047    2048    2049    2050    2051    2052    2053
  151  THRU    160          2054    2055    2056    2057    2058    2059    2065    2066    2067    2070
  161  THRU    164          2071    2072    2073    2074
CONDUCTOR ANALYSIS...  LINEAR =    22,  RADIATION =   142,  TOTAL =   164,  CONNECTIONS =   716

BCD 3CONSTANTS DATA
    NLOOP,5000,DRLXCA,.010,ARLXCA,.010,DAMPA,.5,DAMPD,.5
END
CONSTANTS ANALYSIS...  USER =     0,  ADDED =     0       0       0,  TOTAL =     0


BCD 3ARRAY DATA
REM NODE ORDER FOR POWER DISTRIBUTION IS      25, 26, 27, 28,
REM 21, 22, 23, 24, 101, 102, 103, 104, 105, 106, 107, 108, 109,
REM 110, 111, 112, 113, 114, 115, 116, 9, 10, 11, 12, 13, 14, 15
REM 16, 29, 30, 31, 32, 17, 18, 19, 20
REM HEAT INPUTS FOR A 1 AMP BEAM CURRENT (BTU/HR)
    1, 2.56, 2.56, 2.56, 2.56, 7.69, 7.69, 7.69, 7.69
       2.05, 2.05, 2.05, 2.05, 8.20, 8.20, 8.20, 8.20
       10.25, 10.25, 10.25, 10.25, 102.5, 102.5, 102.5, 102.5
       19.73, 19.73, 19.73, 19.73, 2.05, 2.05, 2.05, 2.05
       16.41, 16.41, 16.41, 16.41, 2.56, 2.56, 2.56, 2.56,END
REM HEAT INPUTS FOR A 2 AMP BEAM CURRENT (BTU/HR)
    2, 4.27, 4.27, 4.27, 4.27, 12.8, 12.8, 12.8, 12.8
       3.4, 3.4, 3.4, 3.4, 13.65, 13.65, 13.65, 13.65
       17.07, 17.07, 17.07, 17.07, 170.7, 170.7, 170.7, 170.7
       32.87, 32.87, 32.87, 32.87,  3.4, 3.4, 3.4, 3.4
       27.3, 27.3, 27.3, 27.3, 4.27, 4.27, 4.27, 4.27,END
REM HEAT INPUTS FOR A .5 AMP BEAM CURRENT (BTU/HR)
    4, 1.28, 1.28, 1.28, 1.28, 3.85, 3.85, 3.85, 3.85
       1.03, 1.03, 1.03, 1.03, 4.10, 4.10, 4.10, 4.10
       5.12, 5.12, 5.12, 5.12, 51.2, 51.2, 51.2, 51.2
       9.87, 9.87, 9.87, 9.87, 1.03, 1.03, 1.03, 1.03
       8.20, 8.20, 8.20, 8.20, 1.28, 1.28, 1.28, 1.28,END
REM NODE ORDER FOR SOLAR FLUX IS 85, 86, 87, 88, 25, 26, 27, 28,
REM 29, 30, 31, 32
REM SOLAR INPUTS FOR 1 SUN INTENSITY
REM THESE VALUES ARE DOUBLED FOR 2 SUNS INTENSITY
    3,30.0, 30.0, 30.0, 30.0, 18.4, 18.4, 18.4, 18.4
    20.0, 20.0, 20.0, 20.0,END
END
ARRAY ANALYSIS...  NUMBER OF ARRAYS =     4  TOTAL LENGTH =    136
```

Execution Procedure

```
     BCD 3EXECUTION
    DIMENSION X(5000)                                                    F
    NDIM=5000                                                            F
    NTH=0                                                                F
    DIMENSION E1(1000) ,E2(1000),AREA1(1000),AREA2(1000),F12(1000)       F
     REM
     REM E1 ARRAY
     REM
    DATA (E1(I),I=23,164) / 52*.6, 40*.15, .8, .775, .7, .675, 8*.15,    F
   1 .175, .15, .15, .275, 8*.15, .3, 25*.15  /                          F
     REM
     REM E2 ARRAY
     REM
```

```
      DATA (E2(I),I=23,164) /  16*.60, 76*.15,                          F
     1 42*1., 3*1., 5*1.  /                                             F
        REM
        REM AREA1 ARRAY (SQUARE INCHES)
        REM
      DATA (AREA1(I),I=23,164) / 9.28, 12.2, 9.28, 12.2, 9.28, 12.2,    F
     1 2*9.28, 2*12.2, 7*9.28, 2*12.2, 2*9.28, 2*12.2, 2*9.28, 2*12.2,  F
     2 2*9.28, 2*12.2, 2*9.28, 2*12.2, 2*9.28, 2*12.2, 2*9.28, 2*12.2,  F
     3 2*9.28, 2*12.2, 2*9.28, 2*12.2,   9.28,                          F
     4   9.28, 2*12.2, 2*9.28, 2*12.2, 2*9.28, 12.2, 9.28, 12.2,        F
     5 8*6.8, 3*12.7, 12.2, 19., 12.7, 2*13.8, 104.6, 2*12.1, 45.4,     F
     6 2*3.98, 2*4.4, 12.1, 104.6, 12.1, 104.6,                         F
     7 9.28, 2*12.2, 9.28,                    4*104.6, 4*12.1, 6.8,2*12.8,F
     8 45.2, 4*33.1, 4*8.0, 28.8,                                       F
     9 8*33.1, 8*8.0,  33.1, 104.6,                                     F
     A 12.1, 4.4,              8.0,  29.8, 29.8, 2*4.4  /               F
        REM
        REM AREA2 ARRAY (SQUARE INCHES)
        REM
      DATA (AREA2(I),I=23,164) / 9.28, 12.2, 9.28, 10*12.2, 3*9.28,     F
     1 12*6.77, 12*12.7, 12*34.7,                   8*43.5, 4*12.1,     F
     2 3*34.7, 3*12.7, 2*6.8, 3*34.7, 22.1, 38.3, 12.7, 2*12.1, 33.1,   F
     3 8.0, 6.13, 252., 2*12.1, 2*8.0, 8.0, 33.1, 8.0, 33.1, 42*140.,   F
     4 8*140.  /                                                        F
        REM
        REM INTERNAL VIEW FACTORS
        REM
      DATA (F12(I),I=23,114) / .021, .027, .021, .028, .017, .016, .026, F
     1 .027, .026, .027, .0093, .021, .025, .0044, .013, .017, .0022,   F
     2 .0035, .0059, .0088, .0084, .0105, .013, .0149, .0117, .0133,    F
     3 .0148, .0156, .0296, .044, .071, .110, .022, .025, .026, .027,   F
     4 .0155, .0155, .0137, .010, .437, .266, .153, .096, .043, .059,   F
     5 .060, .054, .010, .029, .035, .037, 1., 1., 1., .5, .0074, .0075,F
     6 .0073, .0038, .50, .0098, .0038,.00028, .048, .038, .048,        F
     7       .166, .023, .006, .016, .016, .0785, .0425, .025,          F
     8 .108, .0041, 1., .22, .006, .302, .160, .23, 1., .55, .009, .39, F
     9 .003, .008, .020, .008, .020  /                                  F
        REM
        REM EXTERNAL VIEW FACTORS
        REM
      DATA (F12(I),I=115,164) / .0891, .1095, .137, .174,               F
     1                    3*.30,.30, 3*.16,.16,.217, .5, 1., .15,       F
     2 3*.84, .84, 3*.71, .71, 1.,                                      F
     3 .04, .04, 3*.04, .04, 2*.04, .031, .031, 3*.031, .031, 2*.031,   F
     4 .04,                          .05,.05,.08, .24, .15, .15, .39, .39/F
        REM
        REM CALCULATE AND PRINT RADIATION CONDUCTOR VALUES (BTU/HR.R**4)
        REM USING THE VALUES IN THE ABOVE ARRAYS
        REM
      DO 300 I=23,164                                                   F
      IF(G(I).NE.0.) G(I)=1.                                            F
  300 CONTINUE                                                          F
      DO 100 I=23,164                                                   F
      G(I)=G(I)*1.19E-11*AREA1(I)*(1./((1./E1(I)-1.)+AREA1(I)/AREA2(I)) F
     1 *(1./E2(I)-1.)+1./F12(I)))                                       F
  100 CONTINUE                                                          F
      WRITE(6,101)                                                      F
  101 FORMAT(1H1,10X,1HI,5X,2HE1,5X,2HE2,5X,5HAREA1,5X,5HAREA2,8X,      F
     1 3HF12,8X,1HG)                                                    F
```

```
      WRITE(6,102) (I,E1(I),E2(I),AREA1(I),AREA2(I),F12(I),G(I),I=23,164    F
     1)                                                                     F
  102 FORMAT(I13,2F6.2,F11.4,F10.4,2E14.4)                                  F
       REM CALCULATE STEADY STATE TEMPERATURES
           CINDSS
       REM PRINT THRUSTER HEAT INPUTS
           QIPRNT
       END
       BCD 3VARIABLES 1
       REM
       REM STORE HEAT INPUTS FOR 2 AMP BEAM CURRENT
       REM USE BKARAD(A1+1,ETC.) FOR 1 AMP, BKARAD(A4+1,ETC.) FOR .5 AMP
       REM
           BKARAD(A2+1,            Q25,Q26,Q27,Q28,Q21,Q22,Q23,Q24
           Q101,Q102,Q103,Q104,Q105,Q106,Q107,Q108,Q109,Q110,Q111,Q112
           0113,Q114,Q115,Q116,Q9,Q10,Q11,Q12,Q13,Q14,Q15,Q16,Q29,Q30
           Q31,Q32,Q17,Q18,Q19,Q20)
       REM
       REM ADD BKARAD(A3+1,ETC) FOR SOLAR FLUX WHEN USED
       REM
       END
       BCD 3VARIABLES 2
       END
       BCD 3OUTPUT CALLS
       REM CONVERT TEMPERATURES FROM F TO K
      DO 100 I=1,62                                                         F
      T(I)=5./9.*(T(I)+40.)-40.                                             F
      T(I)=T(I)+273.                                                        F
  100 CONTINUE                                                              F
       REM PRINT TEMPERATURES IN K
           TPRINT
       REM CONVERT TEMPERATURES FROM K TO F
      DO 200 I=1,62                                                         F
      T(I)=T(I)-273.                                                        F
      T(I)=1.8*(T(I)+40.)-40.                                               F
  200 CONTINUE                                                              F
       REM PRINT TEMPERATURES IN F
           TPRINT
       END
```

Radiation Properties and Calculated Radiation Conductors

I	E1	E2	AREA1	AREA2	F12	G
23	.60	.60	9.2800	9.2800	.2100-01	.2256-11
24	.60	.60	12.2000	12.2000	.2700-01	.3784-11
25	.60	.60	9.2800	9.2800	.2100-01	.2256-11
26	.60	.60	12.2000	12.2000	.2800-01	.3919-11
27	.60	.60	9.2800	12.2000	.1700-01	.1841-11
28	.60	.60	12.2000	12.2000	.1600-01	.2274-11
29	.60	.60	9.2800	12.2000	.2600-01	.2786-11
30	.60	.60	9.2800	12.2000	.2700-01	.2890-11
31	.60	.60	12.2000	12.2000	.2600-01	.3648-11
32	.60	.60	12.2000	12.2000	.2700-01	.3784-11
33	.60	.60	9.2800	12.2000	.9300-02	.1016-11
34	.60	.60	9.2800	12.2000	.2100-01	.2263-11
35	.60	.60	9.2800	12.2000	.2500-01	.2682-11

36	.60	.60	9.2800	9.2800	.4400-02	.4831-12
37	.60	.60	9.2800	9.2800	.1300-01	.1411-11
38	.60	.60	9.2800	9.2800	.1700-01	.1836-11
39	.60	.15	9.2800	6.7700	.2200-02	.2395-12
40	.60	.15	12.2000	6.7700	.3500-02	.4895-12
41	.60	.15	12.2000	6.7700	.5900-02	.8049-12
42	.60	.15	9.2800	6.7700	.8800-02	.9047-12
43	.60	.15	9.2800	6.7700	.8400-02	.8663-12
44	.60	.15	12.2000	6.7700	.1050-01	.1366-11
45	.60	.15	12.2000	6.7700	.1300-01	.1654-11
46	.60	.15	9.2800	6.7700	.1490-01	.1462-11
47	.60	.15	9.2800	6.7700	.1170-01	.1176-11
48	.60	.15	12.2000	6.7700	.1330-01	.1667-11
49	.60	.15	12.2000	6.7700	.1480-01	.1651-11
50	.60	.15	9.2800	6.7700	.1560-01	.1522-11
51	.60	.15	9.2800	12.7000	.2960-01	.2862-11
52	.60	.15	12.2000	12.7000	.4400-01	.5034-11
53	.60	.15	12.2000	12.7000	.7100-01	.7189-11
54	.60	.15	9.2800	12.7000	.1100+00	.7946-11
55	.60	.15	9.2800	12.7000	.2200-01	.2197-11
56	.60	.15	12.2000	12.7000	.2500-01	.3149-11
57	.60	.15	12.2000	12.7000	.2600-01	.3257-11
58	.60	.15	9.2800	12.7000	.2700-01	.2639-11
59	.60	.15	9.2800	12.7000	.1550-01	.1593-11
60	.60	.15	12.2000	12.7000	.1550-01	.2056-11
61	.60	.15	12.2000	12.7000	.1370-01	.1835-11
62	.60	.15	9.2800	12.7000	.1000-01	.1054-11
63	.60	.15	9.2800	34.7000	.4370+00	.2470-10
64	.60	.15	12.2000	34.7000	.2660+00	.2262-10
65	.60	.15	12.2000	34.7000	.1530+00	.1579-10
66	.60	.15	9.2800	34.7000	.9600-01	.8765-11
67	.60	.15	9.2800	34.7000	.4300-01	.4341-11
68	.60	.15	12.2000	34.7000	.5900-01	.7404-11
69	.60	.15	12.2000	34.7000	.6000-01	.7512-11
70	.60	.15	9.2800	34.7000	.5400-01	.5335-11
71	.60	.15	9.2800	34.7000	.1000-01	.1081-11
72	.60	.15	12.2000	34.7000	.2900-01	.3909-11
73	.60	.15	12.2000	34.7000	.3500-01	.4649-11
74	.60	.15	9.2800	34.7000	.3700-01	.3781-11
75	.15	.15	9.2800	43.5000	.1000+01	.1402-10
76	.15	.15	12.2000	43.5000	.1000+01	.1758-10
77	.15	.15	12.2000	43.5000	.1000+01	.1758-10
78	.15	.15	9.2800	43.5000	.5000+00	.1244-10
79	.15	.15	9.2800	43.5000	.7400-02	.7776-12
80	.15	.15	12.2000	43.5000	.7500-02	.1033-11
81	.15	.15	12.2000	43.5000	.7300-02	.1007-11
82	.15	.15	9.2800	43.5000	.3800-02	.4090-12
83	.15	.15	9.2800	12.1000	.5000+00	.9193-11
84	.15	.15	12.2000	12.1000	.9800-02	.1280-11
85	.15	.15	9.2800	12.1000	.3800-02	.4043-12
86	.15	.15	12.2000	12.1000	.2800-03	.4052-13
87	.15	.15	6.8000	34.7000	.4800-01	.2931-11
88	.15	.15	6.8000	34.7000	.3800-01	.2445-11
89	.15	.15	6.8000	34.7000	.4800-01	.2931-11
90	.15	.15	6.8000	12.7000	.1660+00	.5495-11
91	.15	.15	6.8000	12.7000	.2300-01	.1551-11
92	.15	.15	6.8000	12.7000	.6000-02	.4614-12
93	.15	.15	6.8000	6.8000	.1600-01	.1096-11
94	.15	.15	6.8000	6.8000	.1600-01	.1096-11

95	.15	.15	12.7000	34.7000	.7850-01	.7380-11
96	.15	.15	12.7000	34.7000	.4250-01	.4833-11
97	.15	.15	12.7000	34.7000	.2500-01	.3166-11
98	.15	.15	12.2000	22.1000	.1080+00	.8041-11
99	.15	.15	19.0000	38.3000	.4100-02	.0000
100	.15	.15	12.7000	12.7000	.1000+01	.1225-10
101	.15	.15	13.8000	12.1000	.2200+00	.9848-11
102	.15	.15	13.8000	12.1000	.6000-02	.9185-12
103	.15	.15	104.6000	33.1000	.3020+00	.4630-10
104	.15	.15	12.1000	8.0000	.1600+00	.7028-11
105	.15	.15	12.1000	6.1300	.2300+00	.6792-11
106	.15	.15	45.4000	252.0000	.1000+01	.7028-10
107	.15	.15	3.9800	12.1000	.5500+00	.5066-11
108	.15	.15	3.9800	12.1000	.9000-02	.3992-12
109	.15	.15	4.4000	8.0000	.3900+00	.4614-11
110	.15	.15	4.4000	8.0000	.3000-02	.1530-12
111	.15	.15	12.1000	8.0000	.8000-02	.1034-11
112	.15	.15	104.6000	33.1000	.2000-01	.1692-10
113	.15	.15	12.1000	8.0000	.9000-02	.1034-11
114	.15	.15	104.6000	33.1000	.2000-01	.1692-10
115	.80	1.00	9.2800	140.0000	.8910-01	.9625-11
116	.77	1.00	12.2000	140.0000	.1095+00	.1541-10
117	.70	1.00	12.2000	140.0000	.1370+00	.1879-10
118	.67	1.00	9.2800	140.0000	.1740+00	.1773-10
119	.15	1.00	104.6000	140.0000	.3000+00	.1383-09
120	.15	1.00	104.6000	140.0000	.3000+00	.1383-09
121	.15	1.00	104.6000	140.0000	.3000+00	.1383-09
122	.15	1.00	104.6000	140.0000	.3000+00	.1383-09
123	.15	1.00	12.1000	140.0000	.1600+00	.1208-10
124	.15	1.00	12.1000	140.0000	.1600+00	.1208-10
125	.15	1.00	12.1000	140.0000	.1600+00	.1208-10
126	.15	1.00	12.1000	140.0000	.1600+00	.1208-10
127	.18	1.00	6.8000	140.0000	.2170+00	.8680-11
128	.15	1.00	12.8000	140.0000	.5000+00	.0000
129	.15	1.00	12.8000	140.0000	.1000+01	.2285-10
130	.27	1.00	45.2000	140.0000	.1500+00	.5782-10
131	.15	1.00	33.1000	140.0000	.8400+00	.5744-10
132	.15	1.00	33.1000	140.0000	.8400+00	.5744-10
133	.15	1.00	33.1000	140.0000	.8400+00	.5744-10
134	.15	1.00	33.1000	140.0000	.8400+00	.5744-10
135	.15	1.00	8.0000	140.0000	.7100+00	.1346-10
136	.15	1.00	8.0000	140.0000	.7100+00	.1346-10
137	.15	1.00	8.0000	140.0000	.7100+00	.1346-10
138	.15	1.00	8.0000	140.0000	.7100+00	.1346-10
139	.30	1.00	28.8000	140.0000	.1000+01	.1026-09
140	.15	1.00	33.1000	140.0000	.4000-01	.1284-10
141	.15	1.00	33.1000	140.0000	.4000-01	.1284-10
142	.15	1.00	33.1000	140.0000	.4000-01	.1284-10
143	.15	1.00	33.1000	140.0000	.4000-01	.1284-10
144	.15	1.00	33.1000	140.0000	.4000-01	.1284-10
145	.15	1.00	33.1000	140.0000	.4000-01	.1284-10
146	.15	1.00	33.1000	140.0000	.4000-01	.1284-10
147	.15	1.00	33.1000	140.0000	.4000-01	.1284-10
148	.15	1.00	8.0000	140.0000	.3100-01	.2510-11
149	.15	1.00	8.0000	140.0000	.3100-01	.2510-11
150	.15	1.00	8.0000	140.0000	.3100-01	.2510-11
151	.15	1.00	8.0000	140.0000	.3100-01	.2510-11
152	.15	1.00	8.0000	140.0000	.3100-01	.2510-11
153	.15	1.00	8.0000	140.0000	.3100-01	.2510-11

154	.15	1.00	8.0000	140.0000	.3100-01	.2510-11
155	.15	1.00	8.0000	140.0000	.3100-01	.2510-11
156	.15	1.00	33.1000	140.0000	.4000-01	.1284-10
157	.15	1.00	104.6000	140.0000	.5000-01	.4850-10
158	.15	1.00	12.1000	140.0000	.5000-01	.5610-11
159	.15	1.00	4.4000	140.0000	.8000-01	.2882-11
160	.15	1.00	8.0000	140.0000	.2400+00	.9681-11
161	.15	1.00	29.8000	140.0000	.1500+00	.0000
162	.15	1.00	29.8000	140.0000	.1500+00	.0000
163	.15	1.00	4.4000	140.0000	.3900+00	.6361-11
164	.15	1.00	4.4000	140.0000	.3900+00	.6361-11

Initial and Final Temperatures and Thruster Heat Imputs

```
     SYSTEMS IMPROVED NUMERICAL DIFFERENCING ANALYZER  - - -  SINDA  - - -  UNIVAC-1108 FORTRAN-V VERSION

     30 CM. EMT MODEL (NO HEATER)

**********
TIME=       .00000 DTIME=  0.00000    OSGMIN(     0)=  0.00000    TEMPCC(     0)=  0.00000    RELXCC(     0)=  0.00000

 T   101=  2.99667+02  T   102=  2.99667+02  T   103=  2.99667+02  T   104=  2.99667+02  T   105=  2.99667+02  T   106=  2.99667+02
 T   107=  2.99667+02  T   108=  2.99667+02  T   109=  2.99667+02  T   110=  2.99667+02  T   111=  2.99667+02  T   112=  2.99667+02
 T   113=  2.99667+02  T   114=  2.99667+02  T   115=  2.99667+02  T   116=  2.99667+02  T     9=  2.99667+02  T   10=  2.99667+02
 T    11=  2.99667+02  T    12=  2.99667+02  T    13=  2.99667+02  T    14=  2.99667+02  T    15=  2.99667+02  T    16=  2.99667+02
 T    17=  2.99667+02  T    18=  2.99667+02  T    19=  2.99667+02  T    20=  2.99667+02  T    21=  2.99667+02  T    22=  2.99667+02
 T    23=  2.99667+02  T    24=  2.99667+02  T    25=  2.99667+02  T    26=  2.99667+02  T    27=  2.99667+02  T    28=  2.99667+02
 T    29=  2.99667+02  T    30=  2.99667+02  T    31=  2.99667+02  T    32=  2.99667+02  T    33=  2.99667+02  T    34=  2.99667+02
 T    35=  2.99667+02  T    36=  2.99667+02  T    37=  2.99667+02  T    38=  2.99667+02  T    39=  2.99667+02  T    40=  2.99667+02
 T    74=  2.99667+02  T    75=  2.99667+02  T    76=  2.99667+02  T    77=  2.99667+02  T    85=  2.99667+02  T    86=  2.99667+02
 T    87=  2.99667+02  T    88=  2.99667+02  T    46=  3.72444+02  T   501=  9.30000+01  T   502=  9.30000+01  T   503=  9.30000+01
 T   504=  9.30000+01  T   505=  9.30000+01

**********
TIME=       .00000 DTIME=  0.00000    OSGMIN(     0)=  0.00000    TEMPCC(     0)=  0.00000    RELXCC(     0)=  0.00000

 T   101=  8.00000+01  T   102=  8.00000+01  T   103=  8.00000+01  T   104=  8.00000+01  T   105=  8.00000+01  T   106=  8.00000+01
 T   107=  8.00000+01  T   108=  8.00000+01  T   109=  8.00000+01  T   110=  8.00000+01  T   111=  8.00000+01  T   112=  8.00000+01
 T   113=  8.00000+01  T   114=  8.00000+01  T   115=  8.00000+01  T   116=  8.00000+01  T     9=  8.00000+01  T   10=  8.00000+01
 T    11=  8.00000+01  T    12=  8.00000+01  T    13=  8.00000+01  T    14=  8.00000+01  T    15=  8.00000+01  T    16=  8.00000+01
 T    17=  8.00000+01  T    18=  8.00000+01  T    19=  8.00000+01  T    20=  8.00000+01  T    21=  8.00000+01  T    22=  8.00000+01
 T    23=  8.00000+01  T    24=  8.00000+01  T    25=  8.00000+01  T    26=  8.00000+01  T    27=  8.00000+01  T    28=  8.00000+01
 T    29=  8.00000+01  T    30=  8.00000+01  T    31=  8.00000+01  T    32=  8.00000+01  T    33=  8.00000+01  T    34=  8.00000+01
 T    35=  8.00000+01  T    36=  8.00000+01  T    37=  8.00000+01  T    38=  8.00000+01  T    39=  8.00000+01  T    40=  8.00000+01
 T    74=  8.00000+01  T    75=  8.00000+01  T    76=  8.00000+01  T    77=  8.00000+01  T    85=  8.00000+01  T    86=  8.00000+01
 T    87=  8.00000+01  T    88=  8.00000+01  T    46=  2.11000+02  T   501=-3.10000+02  T   502=-3.10000+02  T   503=-3.10000+02
 T   504=-3.10000+02  T   505=-3.10000+02

**********
TIME=       .00000 DTIME=  0.00000    OSGMIN(     0)=  0.00000    TEMPCC(     0)=  0.00000    RELXCC(    38)=  9.76372-03

 T   101=  5.22481+02  T   102=  5.22481+02  T   103=  5.22481+02  T   104=  5.22481+02  T   105=  5.33286+02  T   106=  5.33286+02
 T   107=  5.33286+02  T   108=  5.33286+02  T   109=  5.45662+02  T   110=  5.45662+02  T   111=  5.45662+02  T   112=  5.45662+02
 T   113=  6.73246+02  T   114=  6.73246+02  T   115=  6.73246+02  T   116=  6.73246+02  T     9=  4.36751+02  T   10=  4.36751+02
 T    11=  4.36751+02  T    12=  4.36751+02  T    13=  5.03312+02  T    14=  5.03312+02  T    15=  5.03312+02  T    16=  5.03312+02
 T    17=  5.33306+02  T    18=  5.33306+02  T    19=  5.33306+02  T    20=  5.33306+02  T    21=  5.61452+02  T    22=  5.61452+02
 T    23=  5.61452+02  T    24=  5.61452+02  T    25=  4.63753+02  T    26=  4.63753+02  T    27=  4.63753+02  T    28=  4.63753+02
 T    29=  5.13838+02  T    30=  5.13838+02  T    31=  5.13838+02  T    32=  5.13838+02  T    33=  3.47247+02  T    34=  3.47247+02
 T    35=  3.47247+02  T    36=  3.47247+02  T    37=  3.40945+02  T    38=  3.40945+02  T    39=  3.40945+02  T    40=  3.40945+02
 T    74=  4.14048+02  T    75=  4.14048+02  T    76=  4.14048+02  T    77=  4.14048+02  T    85=  3.11271+02  T    86=  3.11271+02
 T    87=  3.11271+02  T    88=  7.11271+02  T    46=  3.72444+02  T   501=  9.30000+01  T   502=  9.30000+01  T   503=  9.30000+01
 T   504=  9.30000+01  T   505=  9.30000+01

**********
TIME=       .00000 DTIME=  0.00000    OSGMIN(     0)=  0.00000    TEMPCC(     0)=  0.00000    RELXCC(    38)=  9.76372-03

 T   101=  4.81065+02  T   102=  4.81065+02  T   103=  4.81065+02  T   104=  4.81065+02  T   105=  5.20514+02  T   106=  5.20514+02
 T   107=  5.20514+02  T   108=  5.20514+02  T   109=  5.22791+02  T   110=  5.22791+02  T   111=  5.22791+02  T   112=  5.22791+02
 T   113=  7.52442+02  T   114=  7.52442+02  T   115=  7.52442+02  T   116=  7.52442+02  T     9=  3.26752+02  T   10=  3.26752+02
 T    11=  3.26752+02  T    12=  3.26752+02  T    13=  4.46561+02  T    14=  4.46561+02  T    15=  4.46561+02  T    16=  4.46561+02
 T    17=  5.00551+02  T    18=  5.00551+02  T    19=  5.00551+02  T    20=  5.00551+02  T    21=  5.51214+02  T    22=  5.51214+02
 T    23=  5.51214+02  T    24=  5.51214+02  T    25=  3.75355+02  T    26=  3.75355+02  T    27=  3.75355+02  T    28=  3.75355+02
 T    29=  4.65508+02  T    30=  4.65508+02  T    31=  4.65508+02  T    32=  4.65508+02  T    33=  1.65645+02  T    34=  1.65645+02
 T    35=  1.65645+02  T    36=  1.65645+02  T    37=  1.52682+02  T    38=  1.52682+02  T    39=  1.52682+02  T    40=  1.52682+02
 T    74=  2.85887+02  T    75=  2.85887+02  T    76=  2.85887+02  T    77=  2.85887+02  T    85=  1.00268+02  T    86=  1.00268+02
 T    87=  1.00268+02  T    88=  1.00268+02  T    46=  2.11000+02  T   501=-3.10000+02  T   502=-3.10000+02  T   503=-3.10000+02
 T   504=-3.10000+02  T   505=-3.10000+02

LOOPCT =     90 ENGBAL =    .17661+00

 QI   101=  3.40000+00  QI   102=  3.40000+00  QI   103=  3.40000+00  QI   104=  3.40000+00  QI   105=  1.36500+01  QI   106=  1.36500+01
 QI   107=  1.36500+01  QI   108=  1.36500+01  QI   109=  1.70700+01  QI   110=  1.70700+01  QI   111=  1.70700+01  QI   112=  1.70700+01
 QI   113=  1.70700+02  QI   114=  1.70700+02  QI   115=  1.70700+02  QI   116=  1.70700+02  QI     9=  3.28700+01  QI   10=  3.28700+01
 QI    11=  3.28700+01  QI    12=  3.28700+01  QI    13=  3.40000+00  QI    14=  3.40000+00  QI    15=  3.40000+00  QI    16=  3.40000+00
 QI    17=  4.27000+00  QI    18=  4.27000+00  QI    19=  4.27000+00  QI    20=  4.27000+00  QI    21=  1.26000+01  QI    22=  1.26000+01
 QI    23=  1.26000+01  QI    24=  1.26000+01  QI    25=  4.27000+00  QI    26=  4.27000+00  QI    27=  4.27000+00  QI    28=  4.27000+00
 QI    29=  2.73000+01  QI    30=  2.73000+01  QI    31=  2.73000+01  QI    32=  2.73000+01  QI    33=  0.00000     QI    34=  0.00000
 QI    35=  0.00000     QI    36=  0.00000     QI    37=  0.00000     QI    38=  0.00000     QI    39=  0.00000     QI    40=  0.00000
 QI    74=  0.00000     QI    75=  0.00000     QI    76=  0.00000     QI    77=  0.00000     QI    85=  0.00000     QI    86=  0.00000
 QI    87=  0.00000     QI    88=  0.00000

       END OF DATA
DATA IGNORED - IN CONTROL MODE

$FIN
```

REFERENCES

1. Oglebay, Jon C.: Thermal Analytic Model of a 30-cm Engineering Model Mercury Ion Thruster. NASA TM X-71680, 1975.

2. Wen, L.; Crotty, J. D.; and Pawlik, E. V.: Ion Thruster Characteristics and Performance. AIAA Paper 72-476, Apr. 1972.

3. Wen, L.; and Womack, J. R.: Thruster Array Thermal Control. AIAA Paper 73-1117, Oct. 1973.

4. LM Cathode Thruster System, Supplement. (Hughes Research Labs.; NAS7-100; JPL-952131) NASA CR-110895, 1970.

5. Masek, T. D.: Plasma Properties and Performance of Mercury Ion Thrusters. AIAA Paper 69-256, Mar. 1969.

6. Mirtich, M. J.: Thermal Environmental Testing of a 30-cm Engineering Model Thruster. AIAA Paper 76-1034, Nov. 1976.

7. Mirtich, M. J.: The Effects of Exposure to LN_2 Temperatures and 2.5 Suns Solar Radiation on 30-cm Ion Thruster Performance. AIAA Paper 75-343, Mar. 1975.

8. Kreith, Frank: Principles of Heat Transfer. 2nd ed., International Textbook Co., 1965.

9. Siegel, Robert; and Howell, John R.: Thermal Radiation Heat Transfer. McGraw-Hill Book Co., Inc., 1972, pp. 259-260.

10. Dummer, R. S.; and Breckenridge, W. T., Jr.: Radiation Configuration Factors Program. ERR-AN-224, General Dynamics, 1962.

11. Smith, J. P.: Systems Improved Numerical Differencing Analyzer (SINDA): User's Manual. (TRW-14690-H001-R0-00, TRW Systems Group; NAS9-10435) NASA CR-134271, 1971.

TABLE I. - DESCRIPTION OF THE ANALYTIC NODAL NETWORK

Node	Location	Material
101 - 104	Anode, rear	6Al-4V titanium
105 - 108	Anode, near rear	↓
109 - 112	Anode, near front	↓
113 - 116	Anode, front	↓
9 - 12	Engine body, rear and structure	↓
13 - 16	Engine body, front and ring	6Al-4V titanium and 1010 carbon steel
17 - 20	Pole	1010 carbon steel
21 - 24	Screen grid	Molybdenum
25 - 28	Accelerator grid	Molybdenum
29 - 32	Baseplate	6Al-4V titanium
33 - 36	Ground screen, rear	6061-T6 aluminum
37 - 40	Ground, screen, front	6061-T6 aluminum
46	Rear shield	6061-T6 aluminum
74 - 77	Grid mounting assembly	304 stainless steel
85 - 88	Mask	Pure titanium
501 - 504	Chamber or shield boundary	----------
505	Chamber boundary	----------

TABLE II. - ASSUMED PHYSICAL PROPERTIES OF ION THRUSTER MATERIALS

Material	Density, g/cm^3	Specific heat at 573 K, J/(g)(K)	Thermal conductivity at 573 K, W/(cm)(K)
6061-T6 aluminum	2.77	0.837	1.80
Pure titanium	4.43	.628	.20
Carbon steel	7.81	.544	.60
304 stainless steel	7.92	.523	.20
Molybdenum	10.19	.837	1.20
Tantalum	16.16	.146	.60
Mercury	13.56	.126	.10
Tungsten	19.38	.146	1.50
Alumina (Al_2O_3) (WESGO Al-300)	3.79	.837	.17
Kovar	8.36	.439	.15
6Al-4V titanium	4.43	.628	.10

TABLE III. - ASSUMED SELF-HEATING

POWER DISTRIBUTIONS

Component	Ion beam current, A			Percent of total power
	0.5	1.0	2.0	
	Self-heating power, W			
Accelerator grid	1.5	3.0	5	1.47
Screen grid	4.5	9.0	15	4.42
Anode, rear section	1.2	2.4	4	1.18
Anode, middle sections	10.8	21.6	36.0	10.60
Anode, front section	60.0	120.0	200.0	58.91
Engine body, rear	11.6	23.7	38.5	11.34
Engine body, front	1.2	2.4	4.0	1.18
Baseplate	9.6	19.2	32.0	9.43
Pole	1.5	3.0	5.0	1.47
Total	101.9	203.8	339.5	100.00
Discharge power	111	222	370	------

TABLE IV. - COMPARISON OF EXPERIMENTAL AND ANALYTIC TEMPERATURES[a] FOR THE CALIBRATION TESTS WITH NO SHIELD OR SOLAR INCIDENCE

Component	Ion beam current, A								
	2.0			1.0			0.5		
	T_e, K	T_a, K	Error, $\frac{(T_e - T_a)}{T_e} 100$, percent	T_e, K	T_a, K	Error, $\frac{(T_e - T_a)}{T_e} 100$, percent	T_e, K	T_a, K	Error, $\frac{(T_e - T_a)}{T_e} 100$, percent
Baseplate	513	514	-0.19	467	455	2.57	408	384	5.88
Engine body, rear -									
Under neutralizer housing	---	438	-----	---	388	-----	---	330	----
90° from neutralizer	439	↓	.23	402	↓	3.48	348	↓	5.17
180° from neutralizer	448		2.23	408		4.90	354		6.78
270° from neutralizer	439		.23	402		3.48	349		5.44
Engine body, front -		↓			↓			↓	
Under neutralizer housing[b]	516	504	2.33	465	446	4.09	396	376	5.05
90° from neutralizer	493	↓	-2.23	446	↓	0	378	↓	.53
180° from neutralizer[b]	511		1.37	458		2.62	387		2.84
270° from neutralizer	501	↓	-.60	450	↓	.89	378	↓	.53
Anode, rear	517	523	-1.16	466	462	.86	401	389	2.99
Anode, front	674	673	.15	610	591	3.11	518	494	4.63
Rear shield[c]	373	373	0	356	356	0	317	317	0
Screen mask, 90° from neutralizer	332	312	6.02	310	281	9.35	263	243	7.60
Ground screen, center									
90° from neutralizer	320	349	-9.06	303	307	-1.32	267	259	3.00
180° from neutralizer	332	349	-5.12	311	307	1.29	273	259	5.13
270° from neutralizer	329	349	-6.08	311	307	1.29	272	259	4.08
Average absolute error			2.64			2.80			4.26

[a] T_e = experimental temperature; T_a = analytic temperature.
[b] Thermocouples not on engine body, but on ring near grids.
[c] Set to average experimental values.

TABLE V. - SOLAR HEATING DISTRIBUTION

[$Q_{abs} = NSA\alpha_s$ where N is the number of suns incident, S is the solar constant (= 0.135 W/cm^2), A is the absorbing area, cm^2, and α_s is the effective solar absorptivity.]

Component	Solar Flux				α_s
	1 sun		2 suns		
	Incident, W	Absorbed, W	Incident, W	Absorbed, W	
Mask	76.0	35.2	152.0	70.4	0.46
Accelerator grid	44.9	21.6	89.8	43.2	.48
Baseplate	44.9	23.4	89.8	46.8	.52

TABLE VI. - COMPARISON OF EXPERIMENTAL AND ANALYTIC TEMPERATURES[a] FOR THE CALIBRATION TESTS WITH NO SHIELD AND 2 SUNS SOLAR INCIDENCE

Component	Ion beam current, A								
	2.0			1.0			0.5		
	T_e, K	T_a, K	Error, $\frac{(T_e - T_a)}{T_e}$ 100, percent	T_e, K	T_a, K	Error, $\frac{(T_e - T_a)}{T_e}$ 100, percent	T_e, K	T_a, K	Error, $\frac{(T_e - T_a)}{T_e}$ 100, percent
Baseplate	549	553	-0.73	508	507	0.20	469	461	1.74
Engine body, rear -									
Under neutralizer housing	---	455	------	---	412	------	---	368	------
90° from neutralizer	466	↓	2.36	431	↓	4.41	394	↓	6.60
180° from neutralizer	477	↓	4.61	439	↓	6.15	402	↓	8.46
270° from neutralizer	467	↓	2.57	431	↓	4.41	394	↓	6.60
Engine body, front -		↓			↓			↓	
Under neutralizer housing[b]	548	529	3.47	503	480	4.57	456	430	5.70
90° from neutralizer	527	↓	-.38	482	↓	.41	434	↓	.92
180° from neutralizer[b]	540	↓	2.04	494	↓	2.83	446	↓	3.59
270° from neutralizer	533	↓	.75	486	↓	1.23	436	↓	1.38
Anode, rear	550	550	0	507	498	1.78	463	445	3.89
Anode, front	698	686	1.72	636	609	4.25	554	524	5.42
Rear shield[c]	394	394	0	371	371	0	347	347	0
Screen mask, 90° from neutralizer	468	467	.21	461	458	.65	450	449	.22
Ground screen center									
90° from neutralizer	341	394	-15.54	318	369	-16.04	297	347	-16.84
180° from neutralizer	352	394	-11.93	330	369	-11.82	307	347	-13.03
270° from neutralizer	352	394	-11.93	330	369	-11.82	308	347	-12.66
Average absolute error			4.16			5.04			6.22

[a] T_e = experimental temperature; T_a = analytic temperature.

[b] Thermocouples not on engine body, but on ring near grids.

[c] Set to average experimental values.

TABLE VII. - COMPARISON OF EXPERIMENTAL AND ANALYTIC TEMPERATURES[a] FOR MULTIPLE THRUSTER SIMULATION TESTS

WITH ION-BEAM CURRENT OF 2.0 AMPERES

Component	360^{o} Azimuthal shield						270^{o} Azimuthal shield								
	No sun			2 suns			No sun			1 sun			2 suns		
	Shield temperature, K														
	493			525			483			498			510		
	T_e, K	T_a, K	Error, $\frac{(T_e - T_a)}{T_e} 100$, percent	T_e, K	T_a, K	Error, $\frac{(T_e - T_a)}{T_e} 100$, percent	T_e, K	T_a, K	Error, $\frac{(T_e - T_a)}{T_e} 100$, percent	T_e, K	T_a, K	Error, $\frac{(T_e - T_a)}{T_e} 100$, percent	T_e, K	T_a, K	Error, $\frac{(T_e - T_a)}{T_e} 100$, percent
Baseplate	547	541	1.10	584	581	0.51	539	536	0.56	556	555	0.18	575	574	0.17
Engine body, rear -															
Under neutralizer housing	521	520	.19	553	547	1.08	---	459	-----	---	470	-----	---	478	----
90^{o} from neutralizer	514	↓	-1.17	547	↓	0	499	509	-2.00	513	522	-3.75	529	533	-.76
180^{o} from neutralizer	514	↓	-1.17	549	↓	.36	510	512	-.39	526	525	.19	544	536	1.47
270^{o} from neutralizer	520	↓	0	554	↓	1.26	506	509	-.59	522	522	0	538	533	.93
Engine body, front -															
Under neutralizer housing[b]	558	548	1.79	592	578	2.36	534	521	2.43	551	535	2.90	565	547	3.19
90^{o} from neutralizer	561	↓	2.32	596	↓	3.02	543	540	.55	560	555	.89	575	568	1.22
180^{o} from neutralizer[b]	552	↓	.72	585	↓	1.20	547	542	.91	563	557	1.07	578	570	1.38
270^{o} from neutralizer	553	↓	.90	585	↓	1.20	541	540	.18	557	555	.36	572	568	.70
Anode, rear	550	552	-.36	586	582	.68	542	546	-.74	557	560	-.54	577	574	.52
Anode, front	724	688	4.97	741	703	5.13	696	684	1.72	711	692	2.67	711	699	1.69
Rear shield[c]	450	450	0	476	476	0	440	440	0	451	451	0	464	464	0
Screen mask, 90^{o} from neutralizer	387	377	2.58	498	499	-.20	380	366	3.68	453	440	2.87	504	492	2.38
Ground screen, center -															
90^{o} from neutralizer	485	483	.41	520	522	-.38	477	457	4.19	489	478	2.25	505	494	2.18
180^{o} from neutralizer	478	483	-1.05	510	522	-2.35	479	471	1.67	491	492	-.20	506	508	-.40
270^{o} from neutralizer	481	483	-.42	512	522	-1.95	467	457	2.14	479	478	.21	493	494	-.20
Average absolute error			1.28			1.45			1.55			1.29			1.23

[a] T_e = experimental temperatures; T_a = analytical temperatures.

[b] Thermocouples not on engine body, but on ring near grids.

[c] Set to average experimental values.

TABLE VIII. - COMPARISON OF EXPERIMENTAL AND ANALYTIC TEMPERATURES[a] FOR MULTIPLE THRUSTER SIMULATION TESTS

WITH ION-BEAM CURRENT OF 1.0 AMPERE

Component	360° Azimuthal shield						270° Azimuthal shield								
	No sun			2 suns			No sun			1 sun			2 suns		
	Shield temperature, K														
	468			498			410			446			468		
	T_e, K	T_a, K	Error, $\frac{(T_e - T_a)}{T_e} 100$, percent	T_e, K	T_a, K	Error, $\frac{(T_e - T_a)}{T_e} 100$, percent	T_e, K	T_a, K	Error, $\frac{(T_e - T_a)}{T_e} 100$, percent	T_e, K	T_a, K	Error, $\frac{(T_e - T_a)}{T_e} 100$, percent	T_e, K	T_a, K	Error, $\frac{(T_e - T_a)}{T_e} 100$, percent
Baseplate	498	485	2.61	545	536	1.65	486	469	3.50	509	501	1.57	533	527	1.13
Engine body, rear -															
Under neutralizer housing	477	476	.21	516	506	1.94	---	405	----	---	422	----	---	435	----
90° from neutralizer	471	↓	-1.06	510	↓	.78	445	442	.67	465	467	-.43	487	484	.62
180° from neutralizer	468	↓	-1.71	509	↓	.59	454	444	2.20	475	470	1.05	499	487	2.40
270° from neutralizer	476	↓	0	517	↓	2.13	451	442	2.00	471	467	.85	496	484	2.42
Engine body, front -															
Under neutralizer housing[b]	505	495	1.98	549	532	3.10	476	459	3.57	497	481	3.22	522	498	4.60
90° from neutralizer	506	↓	2.17	550	↓	3.27	480	473	1.46	503	498	.99	529	517	2.27
180° from neutralizer[b]	498	↓	.60	541	↓	1.66	486	475	2.26	508	500	1.57	532	519	2.44
270° from neutralizer	497	↓	.40	539	↓	1.30	478	473	1.05	500	498	.40	525	517	1.52
Anode, rear	498		.60	544	533	2.02	484	478	1.24	507	502	.99	532	522	1.88
Anode, front	641	608	5.15	669	629	5.98	617	600	2.76	633	612	3.32	650	622	4.31
Rear shield[c]	421	421	0	451	451	0	389	389	0	416	416	0	434	434	0
Screen mask, 90° from neutralizer	359	356	.84	486	489	-.62	339	328	3.24	431	421	2.32	486	480	1.23
Ground screen, center -															
90° from neutralizer	454	447	1.54	491	491	0	404	390	3.47	442	431	2.49	465	454	2.37
180° from neutralizer	446	447	-.22	480	491	-2.29	405	401	.99	444	442	.45	465	466	-.22
270° from neutralizer	450	447	.67	482	491	-1.87	397	390	1.76	434	431	.69	455	454	.22
Average absolute error			1.32			1.95			2.16			1.45			1.97

[a] T_e = experimental temperature; T_a = analytic temperature.

[b] Thermocouples not on engine body, but on ring near grids.

[c] Set to average experimental values.

TABLE IX. - COMPARISON OF EXPERIMENTAL AND ANALYTIC TEMPERATURES[a] FOR MULTIPLE THRUSTER SIMULATION TESTS

WITH ION-BEAM CURRENT OF 0.5 AMPERE

Component	360° Azimuthal shield						270° Azimuthal shield								
	No sun			2 suns			No sun			1 sun			2 suns		
	Shield temperature, K														
	413			448			390			410			435		
	T_e, K	T_a, K	Error, $\frac{(T_e - T_a)}{T_e} 100$, percent	T_e, K	T_a, K	Error, $\frac{(T_e - T_a)}{T_e} 100$, percent	T_e, K	T_a, K	Error, $\frac{(T_e - T_a)}{T_e} 100$, percent	T_e, K	T_a, K	Error, $\frac{(T_e - T_a)}{T_e} 100$, percent	T_e, K	T_a, K	Error, $\frac{(T_e - T_a)}{T_e} 100$, percent
Baseplate	441	416	5.67	499	487	2.40	431	406	5.80	459	446	2.83	491	480	2.24
Engine body, rear -															
Under neutralizer housing	421	412	2.14	470	453	3.62	---	352	----	---	374	----	---	391	----
90° from neutralizer	413	↓	.24	462	↓	1.95	397	393	1.47	421	417	.95	449	440	2.00
180° from neutralizer	411	↓	-.24	462	↓	1.95	405	396	2.22	430	420	2.33	459	443	3.49
270° from neutralizer	417	↓	1.20	469	↓	3.41	404	393	2.72	428	417	2.57	457	440	3.72
Engine body, front -		↓			↓										
Under neutralizer housing[b]	439	425	3.19	499	477	4.41	418	396	5.56	446	425	4.73	478	449	6.07
90° from neutralizer	437	↓	2.75	495	↓	3.64	422	412	2.37	449	441	1.78	483	468	3.11
180° from neutralizer[b]	430	↓	1.16	489	↓	2.45	425	413	2.82	453	443	2.21	485	470	3.09
270° from neutralizer	428	↓	.70	485	↓	1.65	416	412	.96	445	441	.90	477	468	1.89
Anode, rear	433	423	2.31	494	↓	3.44	428	412	3.74	456	442	3.07	487	469	3.70
Anode, front	548	512	6.57	587	545	7.16	534	506	5.24	554	523	5.60	578	540	6.57
Rear shield[c]	379	379	0	416	416	0	366	366	0	382	382	0	405	405	0
Screen mask, 90° from neutralizer	317	321	-1.26	466	475	-1.93	313	303	3.19	415	405	2.41	473	469	.85
Ground screen, center -															
90° from neutralizer	396	387	2.27	446	445	.22	384	353	8.07	405	393	2.96	433	422	2.54
180° from neutralizer	388	387	.26	435	445	-2.30	384	364	5.21	405	403	.49	431	433	-.46
270° from neutralizer	394	387	1.78	437	445	-1.83	377	353	6.37	397	393	1.01	423	422	.24
Average absolute error			2.12			2.82			3.98			2.42			2.86

[a] T_e = experimental temperature; T_a = analytic temperature.

[b] Thermocouples not on engine body, but on ring near grids.

[c] Set to average experimental values.

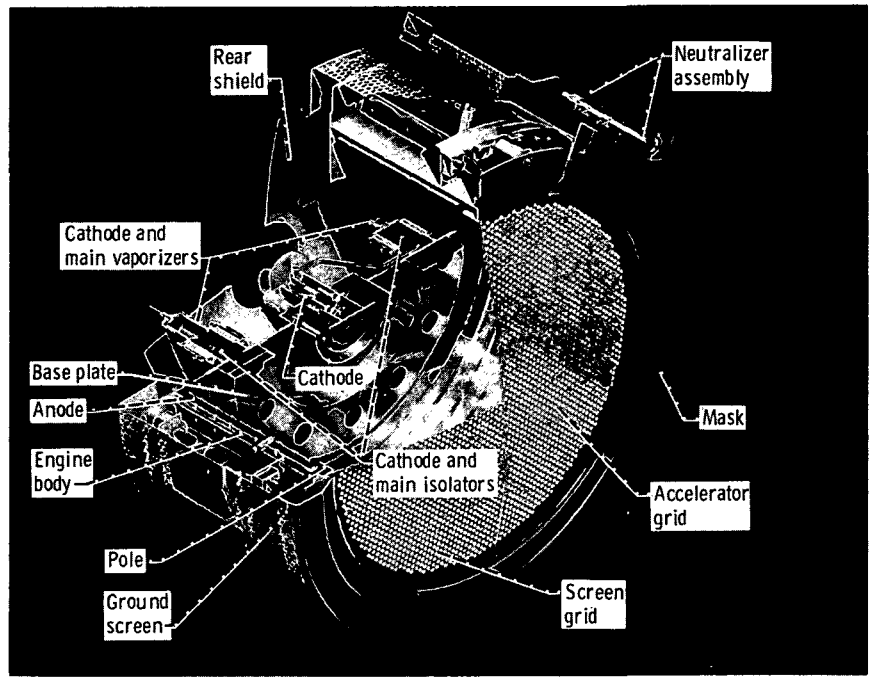

Figure 1. - Cutaway view of 30-centimeter-engineering model thruster.

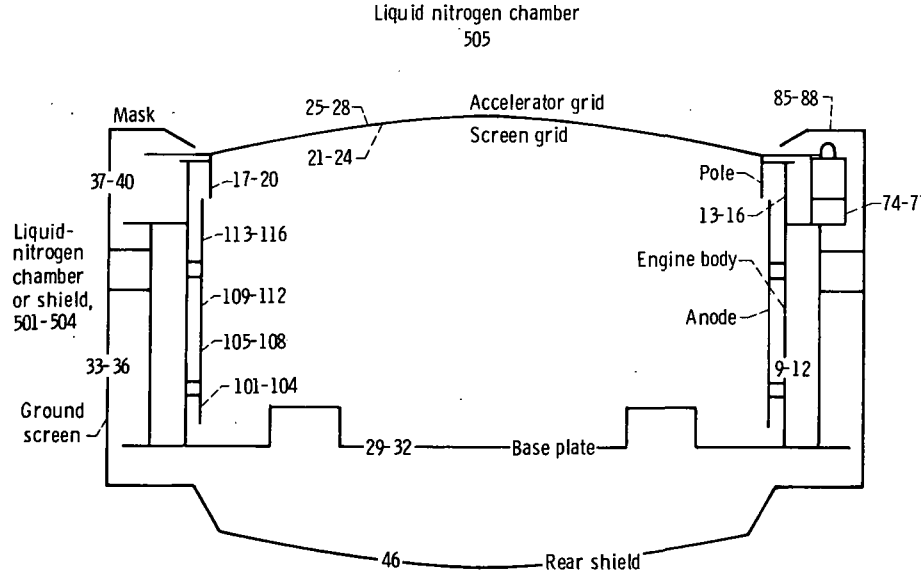

Figure 2. - Simplified engineering model thruster nodal network.

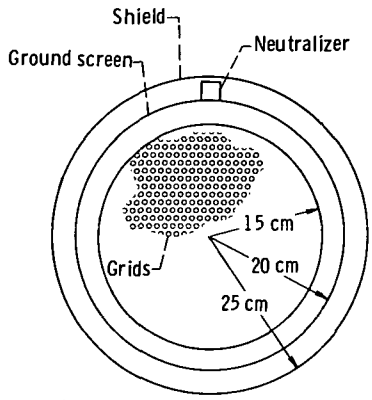

Figure 3. - Schematic of 30-centimeter diameter ion thruster with 360° azimuthal shield.

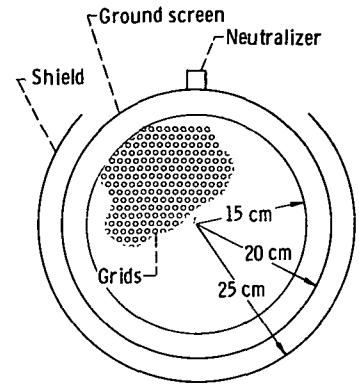

Figure 4. - Schematic of 30-centimeter diameter ion thruster with 270° azimuthal shield.

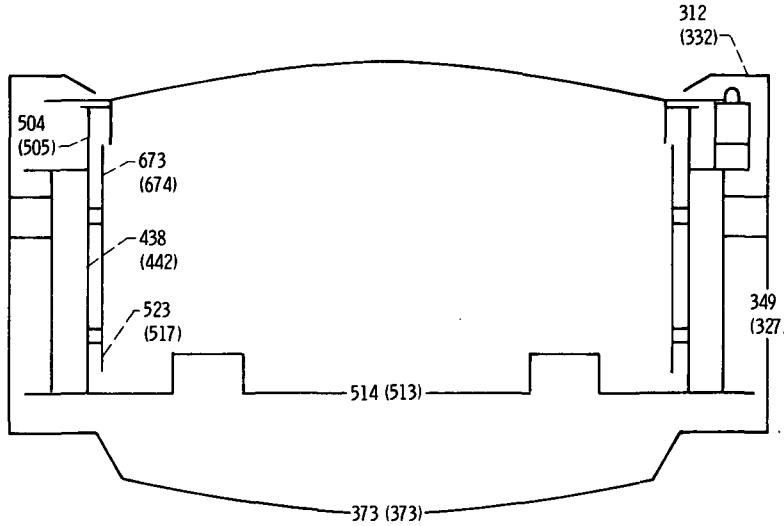

Figure 5. - Analytic and experimental (in parentheses) temperatures (kelvins) for 2-ampere beam current with no shield or solar incidence.

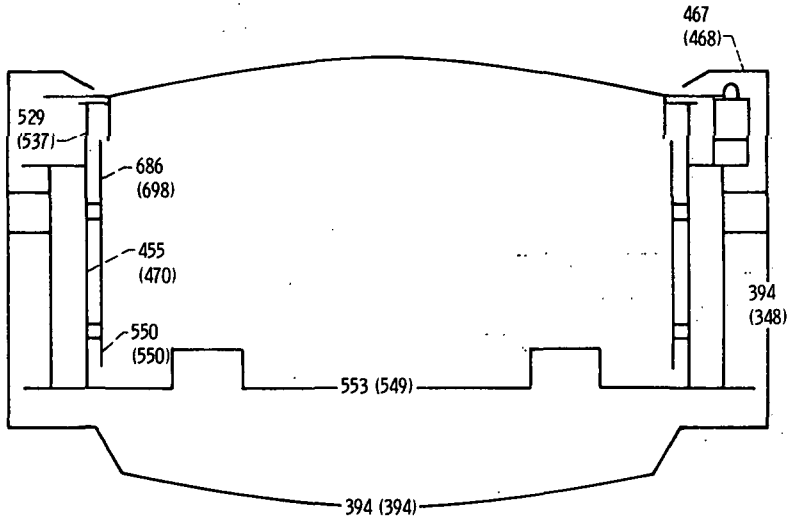

Figure 6. - Analytic and experimental (in parentheses) temperatures (kelvins) for 2-ampere beam current with no shield and 2 suns solar incidence.

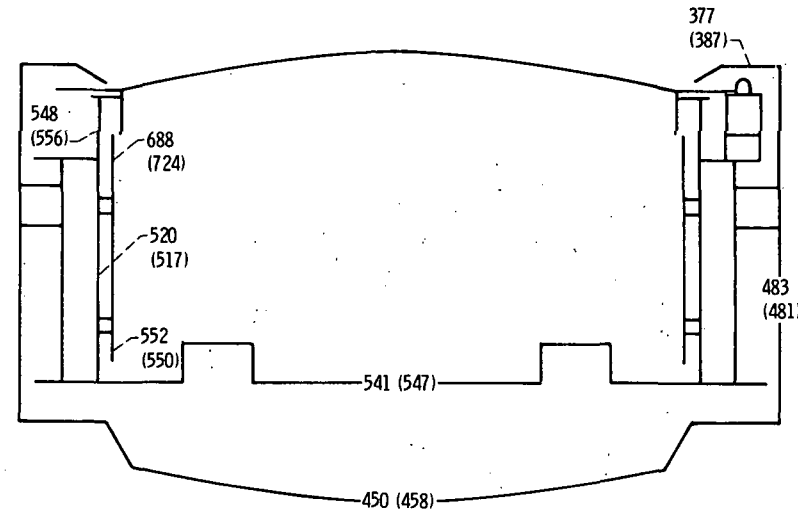

Figure 7. - Analytic and experimental (in parentheses) temperature (kelvins) for 2-ampere beam current with 360^0 azimuthal shield at 493 K and no solar incidence.

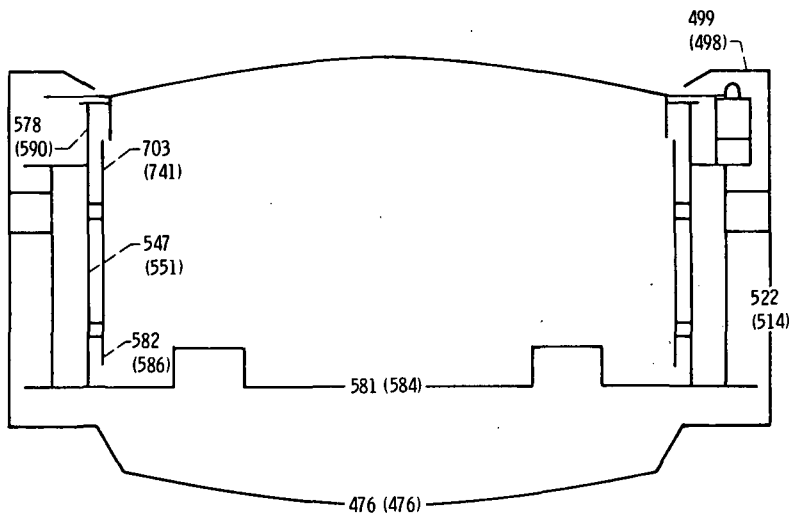

Figure 8. - Analytic and experimental (in parentheses) temperatures (kelvins) for 2-ampere beam current with 360^0 azimuthal shield at 525 K and 2 suns solar incidence.

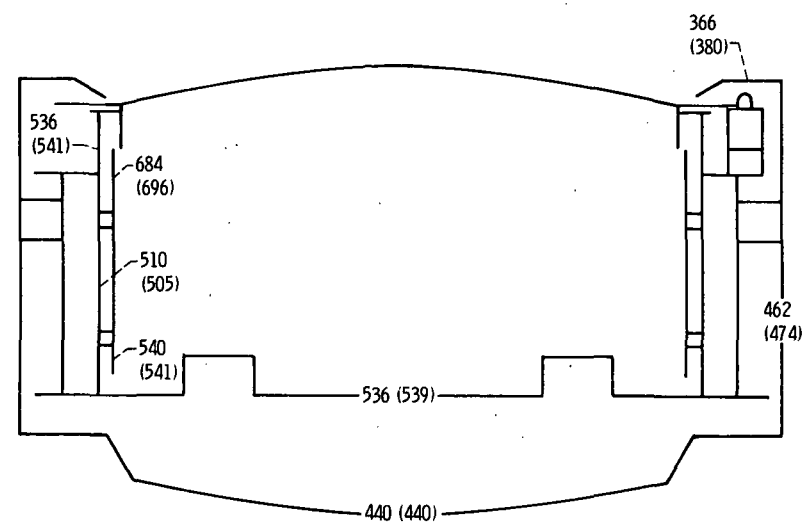

Figure 9. - Analytic and experimental (in parentheses) temperatures (kelvins) for 2-ampere beam current with 270^0 azimuthal shield at 483 K and no solar incidence.

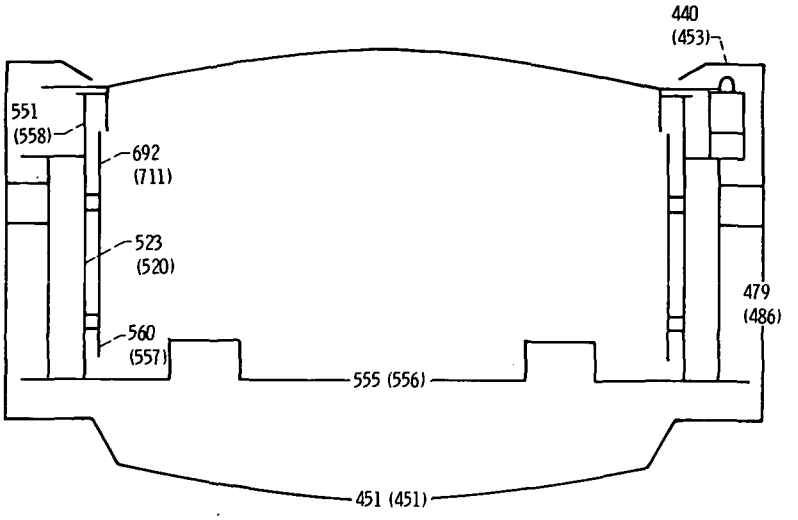

Figure 10. - Analytic and experimental (in parentheses) temperatures (kelvins) for 2-ampere beam current with 270^0 azimuthal shield at 498 K and 1 sun solar incidence.

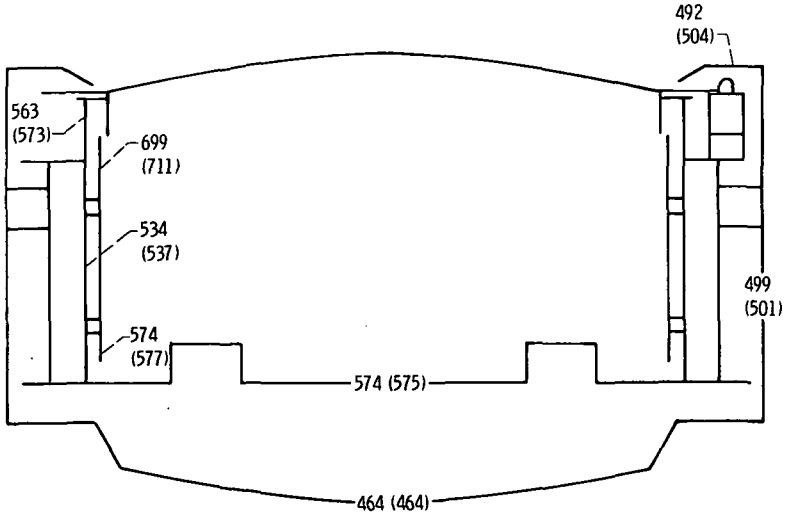

Figure 11. - Analytic and experimental (in parentheses) temperatures (kelvins) for 2-ampere beam current with 270^0 azimuthal shield at 464 K and 2 suns solar incidence.

NATIONAL AERONAUTICS AND SPACE ADMINISTRATION
WASHINGTON, D.C. 20546

OFFICIAL BUSINESS
PENALTY FOR PRIVATE USE $300

SPECIAL FOURTH-CLASS RATE
BOOK

POSTAGE AND FEES PAID
NATIONAL AERONAUTICS AND
SPACE ADMINISTRATION
451

U.S.MAIL

POSTMASTER : If Undeliverable (Section 158 Postal Manual) Do Not Return

"The aeronautical and space activities of the United States shall be conducted so as to contribute . . . to the expansion of human knowledge of phenomena in the atmosphere and space. The Administration shall provide for the widest practicable and appropriate dissemination of information concerning its activities and the results thereof."

—NATIONAL AERONAUTICS AND SPACE ACT OF 1958

NASA SCIENTIFIC AND TECHNICAL PUBLICATIONS

TECHNICAL REPORTS: Scientific and technical information considered important, complete, and a lasting contribution to existing knowledge.

TECHNICAL NOTES: Information less broad in scope but nevertheless of importance as a contribution to existing knowledge.

TECHNICAL MEMORANDUMS: Information receiving limited distribution because of preliminary data, security classification, or other reasons. Also includes conference proceedings with either limited or unlimited distribution.

CONTRACTOR REPORTS: Scientific and technical information generated under a NASA contract or grant and considered an important contribution to existing knowledge.

TECHNICAL TRANSLATIONS: Information published in a foreign language considered to merit NASA distribution in English.

SPECIAL PUBLICATIONS: Information derived from or of value to NASA activities. Publications include final reports of major projects, monographs, data compilations, handbooks, sourcebooks, and special bibliographies.

TECHNOLOGY UTILIZATION PUBLICATIONS: Information on technology used by NASA that may be of particular interest in commercial and other non-aerospace applications. Publications include Tech Briefs, Technology Utilization Reports and Technology Surveys.

Details on the availability of these publications may be obtained from:

SCIENTIFIC AND TECHNICAL INFORMATION OFFICE

NATIONAL AERONAUTICS AND SPACE ADMINISTRATION

Washington, D.C. 20546